JOURNAL OF QUATERNARY SCIENCE (2006) **21**(4) 321–334

Published online 28 March 2006 in Wiley InterScience (www.interscience.wiley.com). DOI: 10.1002/jqs.996

Constraining the age of Lateglacial and early Holocene pollen zones and tephra horizons in southern Sweden with Bayesian probability methods

B. WOHLFARTH,[1]* M. BLAAUW,[2] S. M. DAVIES,[3] M. ANDERSSON,[1] S. WASTEGÅRD,[1] A. HORMES[4] and G. POSSNERT[4]
[1]Department of Physical Geography and Quaternary Geology, Stockholm University, Stockholm, Sweden
[2]Centro de Investigación en Matemáticas, Guanajuato, Mexico
[3]Department of Geography, University of Wales Swansea, Swansea, UK
[4]Ångström Laboratory, Uppsala University, Uppsala, Sweden

Wohlfarth, B., Blaauw, M., Davies, S. M., Andersson, M., Wastegård, S., Hormes, A. and Possnert, G. 2006. Constraining the age of Lateglacial and early Holocene pollen zones and tephra horizons in southern Sweden with Bayesian probability methods. *J. Quaternary Sci.*, **Vol. 21** pp. 321–334. ISSN 0267–8179.

Received 17 July 2004; Revised 28 October 2005; Accepted 9 November 2005

ABSTRACT: The sediment sequence from Hässeldala port in southeastern Sweden provides a unique Lateglacial/early Holocene record that contains five different tephra layers. Three of these have been geochemically identified as the Borrobol Tephra, the Hässeldalen Tephra and the 10-ka Askja Tephra. Twenty-eight high-resolution ^{14}C measurements have been obtained and three different age models based on Bayesian statistics are employed to provide age estimates for the five different tephra layers. The chrono- and pollen stratigraphic framework supports the stratigraphic position of the Borrobol Tephra as found in Sweden at the very end of the Older Dryas pollen zone and provides the first age estimates for the Askja and Hässeldalen tephras. Our results, however, highlight the limitations that arise in attempting to establish a robust, chronologically independent lacustrine sequence that can be correlated in great detail to ice core or marine records. Radiocarbon samples are prone to error and sedimentation rates in lake basins may vary considerably due to a number of factors. Any type of valid and 'realistic' age model, therefore, has to take these limitations into account and needs to include this information in its prior assumptions. As a result, the age ranges for the specific horizons at Hässeldala port are large and calendar year estimates differ according to the assumptions of the age-model. Not only do these results provide a cautionary note for over-dependence on one age-model for the derivation of age estimates for specific horizons, but they also demonstrate that precise correlations to other palaeoarchives to detect leads or lags is problematic. Given the uncertainties associated with establishing age–depth models for sedimentary sequences spanning the Lateglacial period, however, this exercise employing Bayesian probability methods represents the best possible approach and provides the most statistically significant age estimates for the pollen zone boundaries and tephra horizons. Copyright © 2006 John Wiley & Sons, Ltd.

KEYWORDS: Lateglacial; early Holocene; Borrobol Tephra; Hässeldalen Tephra; 10-ka Askja Tephra; Bayesian age–depth modelling; pollen stratigraphy; southeast Sweden.

Introduction

The Weichselian Lateglacial and the early Holocene were characterised by rapid, short-term climatic variations, seen in numerous geological archives around the Northern Hemisphere. Hypotheses to explain these rapid climate fluctuations, which had a distinct impact on terrestrial and marine environments, focus on internal factors (e.g. changes in the thermohaline circulation) (Björck *et al.*, 1996; Broecker, 1998, 2003; Hughen *et al.*, 1998, 2000) as well as external factors (e.g. solar forcing) (Björck *et al.*, 2001; Bond *et al.*, 2001; Goslar *et al.*, 2000; Renssen *et al.*, 2000; van der Plicht *et al.*, 2004). However, to understand the trigger or forcing mechanism that may have initiated these rapid climate changes, it is crucial to map their spatial occurrence and timing and to link the changes observed in different archives on a common and high-resolution timescale. This approach would help decipher the environmental impact of climatic fluctuations in different regions and would enable the testing of hypotheses of synchroneity/asynchroneity between different records.

* Correspondence to: B. Wohlfarth, Department of Physical Geography and Quaternary Geology, Stockholm University, 106 91 Stockholm, Sweden.
E-mail: Barbara.Wohlfarth@geo.su.se

This seemingly straightforward procedure is, however, limited by problems of radiocarbon dating marine and terrestrial sequences during this time interval (e.g., Gulliksen *et al.*, 1998; Lowe and Walker, 2000; Björck and Wohlfarth, 2001; Björck *et al.*, 2003) and by the paucity of annually resolved archives. Recommendations by the INTIMATE group[1] to solve some of these issues include the use of the Greenland Ice Core (GRIP) event stratigraphy as a template and the search for time-synchronous tephra horizons in ice cores and marine and terrestrial records (Björck *et al.*, 1998; Walker *et al.*, 1999; Lowe *et al.*, 2001; Walker, 2001). By correlating chronologically well-constrained sequences to the GRIP template, leads or lags in environmental response as inferred from palaeoarchives in different regions may be evaluated.

Techniques for the detection of tephra layers have changed considerably over the last 10 years with the detection of cryptotephras (Lowe and Hunt, 2001) (horizons that contain a low concentration of volcanic glass shards, all or most of which are <100 μm in size) in areas far more distal to the source volcanoes than previously realised. Cryptotephras can be used as time-synchronous marker horizons if the fallout occurred within one or two years, there has been no reworking or geochemical alteration of the volcanic ash after deposition and the tephras have well characterised geochemical signatures. The introduction of extraction techniques, particularly a density separation method for minerogenic sediments (Turney, 1998b) has greatly extended the geographical distribution of some Lateglacial rhyolitic tephras that were previously delimited by visible occurrences in proximal areas. For instance, the Vedde Ash (10 300 ^{14}C yr BP; Birks *et al.*, 1996; Wastegård *et al.*, 1998) has now been traced into lacustrine sediments in Scotland, Sweden, Arctic Norway, northwest Russia and the Netherlands (Turney *et al.*, 1997; Wastegård *et al.*, 1998, 2000a,b; Davies *et al.*, 2005; Pilcher *et al.*, 2005). In addition, careful examination of sequences has revealed the presence of new, previously undetected tephras that are currently only identified in cryptotephra form. One such example is the Borrobol Tephra, initially identified in Scottish lacustrine sequences (Turney *et al.*, 1997) but subsequently detected within marine sediments from the Icelandic plateau (Eiriksson *et al.*, 2000) and terrestrial records in southern Sweden—one of which is under investigation here (Davies *et al.*, 2003). The discovery of the Borrobol Tephra not only provides an additional marker horizon for correlation purposes during the early Lateglacial but adds considerably to our knowledge of the European tephrochronology framework during this time. A number of other so-called 'new' tephras of Lateglacial age have been identified in the last few years (e.g. Eiriksson *et al.*, 2000; Haflidason *et al.*, 2000; Davies *et al.*, 2003; Mortensen *et al.*, 2005), and thus at present over 30 tephras from the four main volcanic provinces in Europe, are potentially available for precise correlation of terrestrial, marine and ice-core sequences that span the Lateglacial and early Holocene (Davies *et al.*, 2002).

The application of tephrochronology, however, is not without problems, as exemplified by the Lateglacial/early Holocene lake sediment sequence discovered at Hässeldala port in southernmost Sweden (Fig. 1). This 77 cm long sequence provides a unique Lateglacial record containing five distinct tephra layers, three of which have been geochemically identified as the Borrobol Tephra (BT), the Hässeldalen Tephra (HDT) and the 10-ka Askja Tephra (AsT) (Davies *et al.*, 2003). The remaining geochemically unidentified tephra horizons have been tentatively assigned to the Laacher See and Vedde Ash fallout, respectively (Davies *et al.*, 2003). In a previous publication we presented arguments, based on pollen and radiocarbon evidence, for an age assignment of the BT at the late Older Dryas/very early Allerød (GI-1d/GI-1c) boundary (Davies *et al.*, 2004b), which contrasts with British and Icelandic records indicating tephra deposition around the Oldest Dryas/Bølling transition (GS-2/GI-1) (Turney *et al.*, 1997; Lowe *et al.*, 1999; Eiriksson *et al.*, 2000). This age discrepancy has raised the possibility that there may have been more than one BT, indistinguishable by major element geochemistry, deposited during this time interval (Davies *et al.*, 2004b). Indeed, recently published evidence for a 'Borrobol-like tephra' horizon in a Scottish lake sediment sequence dating to ca. 13 610 cal. yr BP and attributed to the early Allerød (Ranner *et al.*, 2005), seems to lend support to this hypothesis. The possible presence of two geochemically identical ash layers during this time period emphasises that regional tephrochronology frameworks need to be underpinned by supplementary geochemical data (e.g. trace and rare earth element analysis) and by a comprehensive chrono- and pollen stratigraphic framework (Turney *et al.*, 2004).

Although the age of the BT as identified at Hässeldala port has been discussed in detail elsewhere (Davies *et al.*, 2004b), the aim of this article is to employ a more comprehensive ^{14}C data set to re-address the BT age estimate and provide ages for the remaining tephras found at this site. First we present a correlation of the local pollen assemblage zones to the regional pollen stratigraphy for southern Sweden, so that the tephra layers are placed within a regional context. Secondly, we employ three different age–depth models based on Bayesian statistics and evaluate their ability to provide a robust chronostratigraphic framework for the tephra layers and the Lateglacial pollen zone boundaries.

Methods

Sediment cores were obtained at Hässeldala port during the spring of 2001 (cores 1 and 2) and during the autumn of 2002 (core 3) with a Russian corer (7.5 cm diameter, 1 m length) (Fig. 1(C)). The cores were wrapped in plastic and kept in cold storage until sampling was undertaken. The first tephrochronological investigations performed on core 1 and reported by Davies *et al.* (2003) clearly showed the potential of the site for further and more detailed investigations. As a follow-up study, sub-sampling for total carbon (TC) was undertaken on cores 1, 2 and 3, terrestrial plant macrofossils for AMS ^{14}C measurements were extracted from core 2 and samples for pollen analysis were taken from core 3. In addition, the stratigraphic position of the cryptotephras was determined for cores 2 and 3 to aid core correlations.

TC was measured in contiguous 1-cm samples using a CS 500 carbon/sulphur analyser. Cryptotephra investigations of the minerogenic Lateglacial sediment followed the density separation method outlined in Turney (1998a) and the more organic early Holocene sediments were subjected to the ashing technique and dilute alkali treatment outlined by Pilcher and Hall (1992), Pilcher *et al.* (1996) and Rose *et al.* (1996), respectively. Samples prepared for microprobe analyses were subjected to an acid digestion technique (Dugmore *et al.*, 1995) and the geochemical results are reported in Davies *et al.* (2003).

Pollen preparation followed the methods outlined in Berglund and Ralska-Jasiewiczowa (1986). Pollen and spores were counted at $\times 400$ magnification and identified with the

[1]INTegration of Ice core Marine and TErrestrial records during the Last Termination—a core programme of the International Union for Quaternary Research (INQUA) Palaeoclimate Commission.

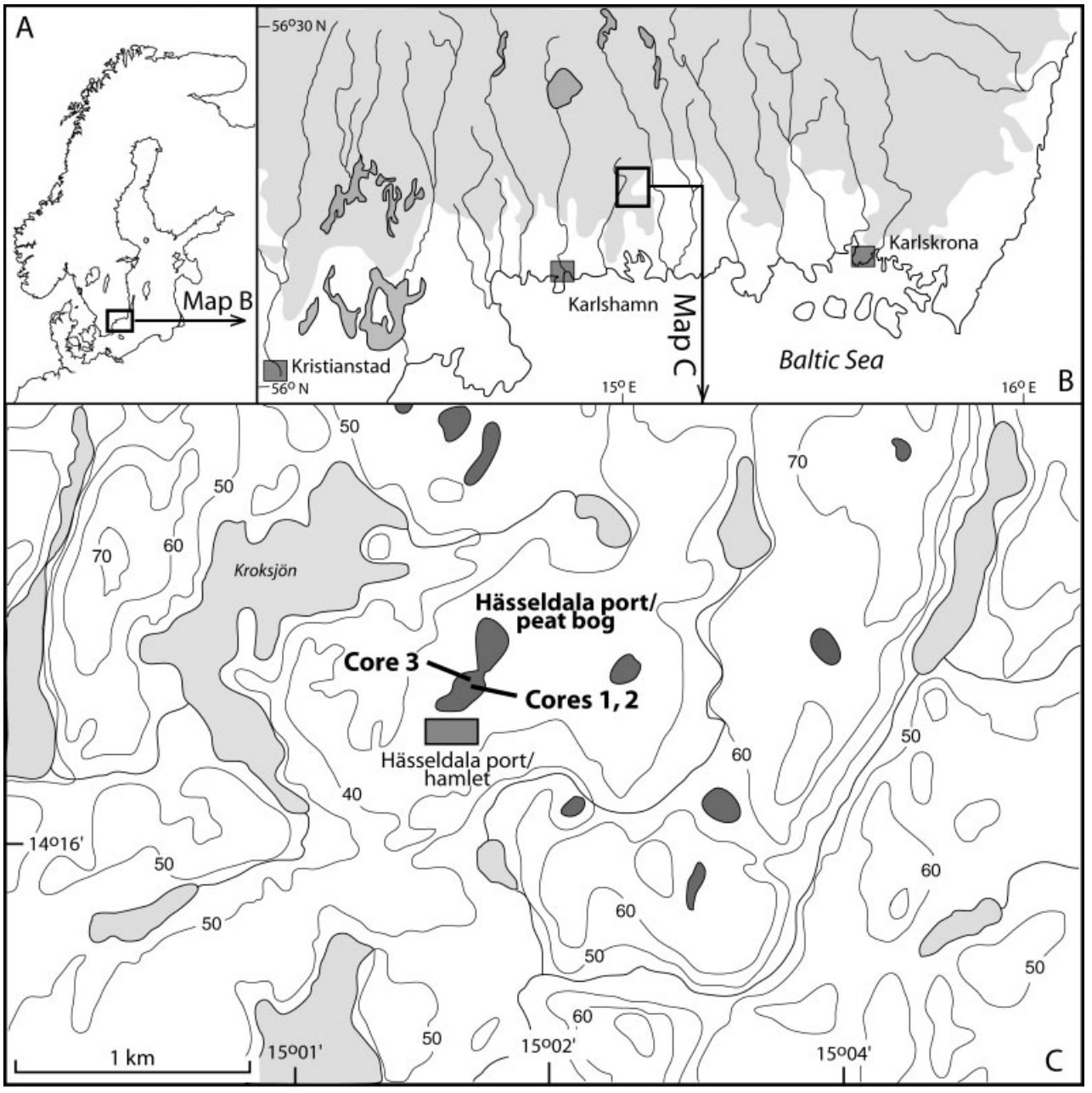

Figure 1 (A) Scandinavia; (B) the location of the site Hässeldala port in southeast Sweden; and (C) topographic map of the site, including coring points 1–3. (B) shaded areas = areas above the Highest Coastline (ca. 60 m a.s.l.); dark grey = lakes. (C) light grey = lakes; dark grey = peat bogs

aid of keys in Moore *et al.* (1991) and in comparison with the reference collections at the Department of Physical Geography and Quaternary Geology, Stockholm University. The pollen diagram was constructed in Tilia and Tilia Graph (Grimm, 1991, 1992) and the local pollen assemblage zones (LPAZ) HÄP 1–7 were established with CONISS (Grimm, 1987).

Sediment slices 1 to 3 cm thick were sieved (0.25 mm mesh) under running water and a low-powered dissecting microscope was used to select and identify terrestrial plant macrofossils. The samples were placed in clean glass bottles, dried at 110 °C and analysed with the EN-tandem accelerator (Possnert, 1990) at Uppsala University. Pre-treatment followed the standard acid–alkali–acid procedure (Björck and Wohlfarth, 2001). However, two of the small samples (Ua-16761 and Ua-16766) were only pretreated with 10% HCl because alkali treatment would have led to loss of material. Prior to the accelerator measurement the dried material (pH 4) was combusted to CO_2 and converted to graphite using a Fe-catalyst reaction. A small fraction of approximately 0.05 mg carbon of the CO_2 gas was used for measurement of the natural mass fractionation, $\delta^{13}C$, in a conventional mass spectrometer (VG OPTIMA).

During periods with highly variable atmospheric ^{14}C concentrations, calibration of individual dates results in very large possible calendar age intervals. To constrain the calibrated ranges, sequences of closely spaced ^{14}C dates can be calibrated simultaneously against the calibration curve IntCal04 (Reimer *et al.*, 2004) in a Bayesian framework using assumptions such as linear accumulation rate or chronological ordering. Three different age-models (A–C) were constructed using Bayesian calibration approaches, which match ^{14}C dates to the IntCal04 calibration curve, using prior information specified below, but excluding biostratigraphical information. Model A (using the software Bpeat) (Blaauw and Christen, 2005) assumes linear accumulation of the entire sequence and a prior probability of 5% of a ^{14}C date being an outlier. ^{14}C measurements derived from corroded plant remains were, however, given a much higher prior outlier probability of 50%. Model B uses the same assumptions as model A, but divides the

^{14}C sequence into three sections, which are wiggle-matched against the radiocarbon calibration curve, allowing for short-lasting hiatuses of up to 100 yr. Bpeat has an in-built dependency of accumulation rates between sections. Given the large possible accumulation rate variations of the sequence, the dependency was here set at very low levels (effectively assuming no dependence of accumulation rates between sections). Model C does not assume linear accumulation, but uses the less stringent assumption of chronological ordering of the dated levels, i.e. the calendar age increases with depth. Prior outlier probabilities were set at 50% for ^{14}C measurements on corroded plant material, and at 5% for the other dates, as in models B and C. Calculations were performed using Bcal (Buck *et al.*, 1999).

Results

Lithostratigraphy, core correlation, tephra horizons and pollen stratigraphy

Cores 1, 2 and 3 were correlated with each other by lithostratigraphy, stratigraphic marker horizons and wiggle-matching of the high-resolution TC curves (Fig. 2). The correlation shows that the sedimentation rates in cores 1 and 2 are comparable, whereas core 3, which is the longest and deepest sequence, has higher sedimentation rates. Such marked differences between nearby sequences are fairly common for small Lateglacial basins in southern Sweden, where erosion and bedrock topography has a strong influence on the sedimentation rate.

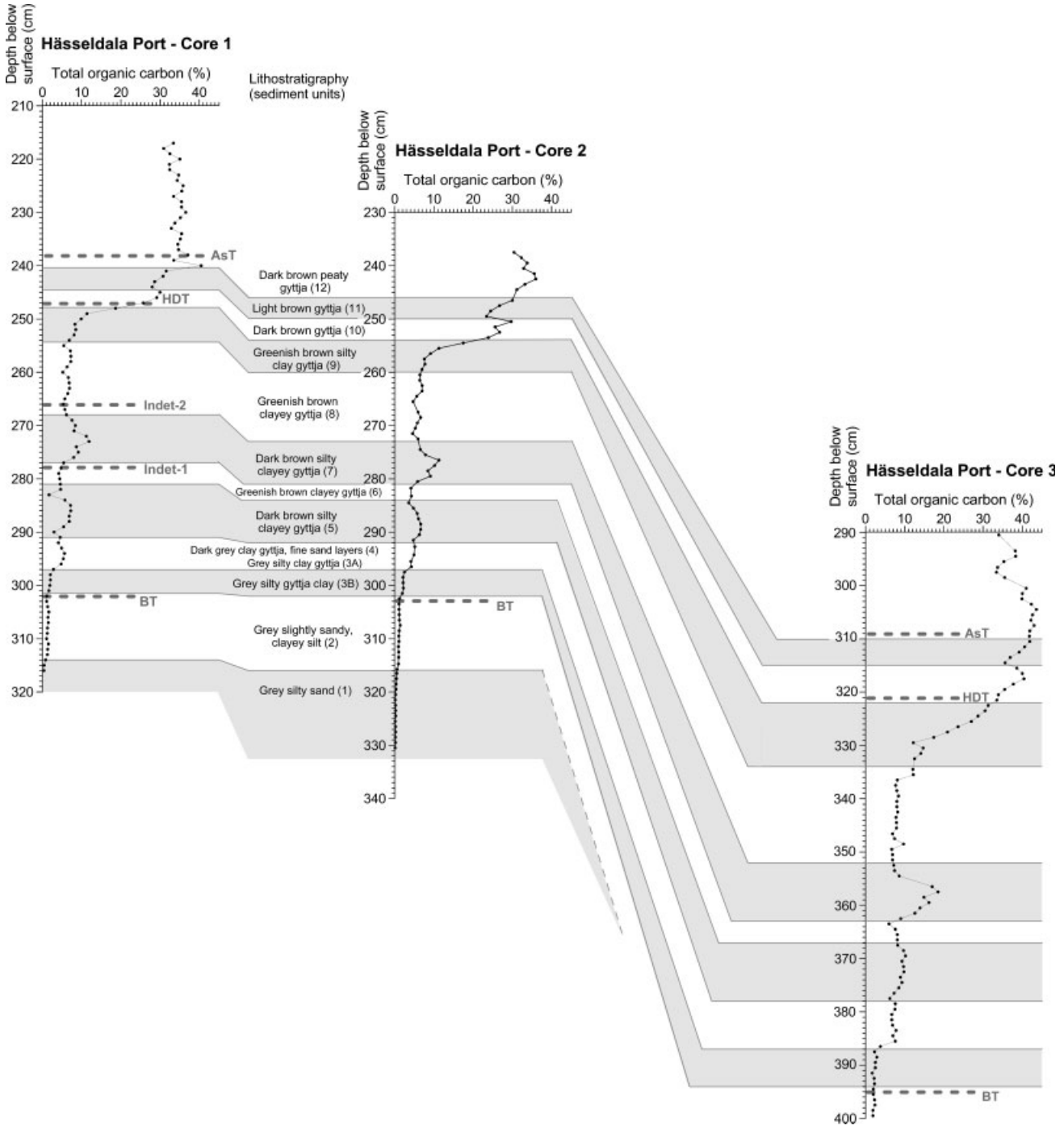

Figure 2 Lithostratigraphy and total organic carbon curves for sediment cores 1, 2 and 3 from Hässeldala port. The correlation between the three cores is based on wiggle-matching the TC curves. The cryptotephra layers found in the three sequences are indicated by dashed lines. BT = Borrobol Tephra, Indet. = unidentified tephra, HDT = Hässeldalen tephra, AsT = Askja Tephra

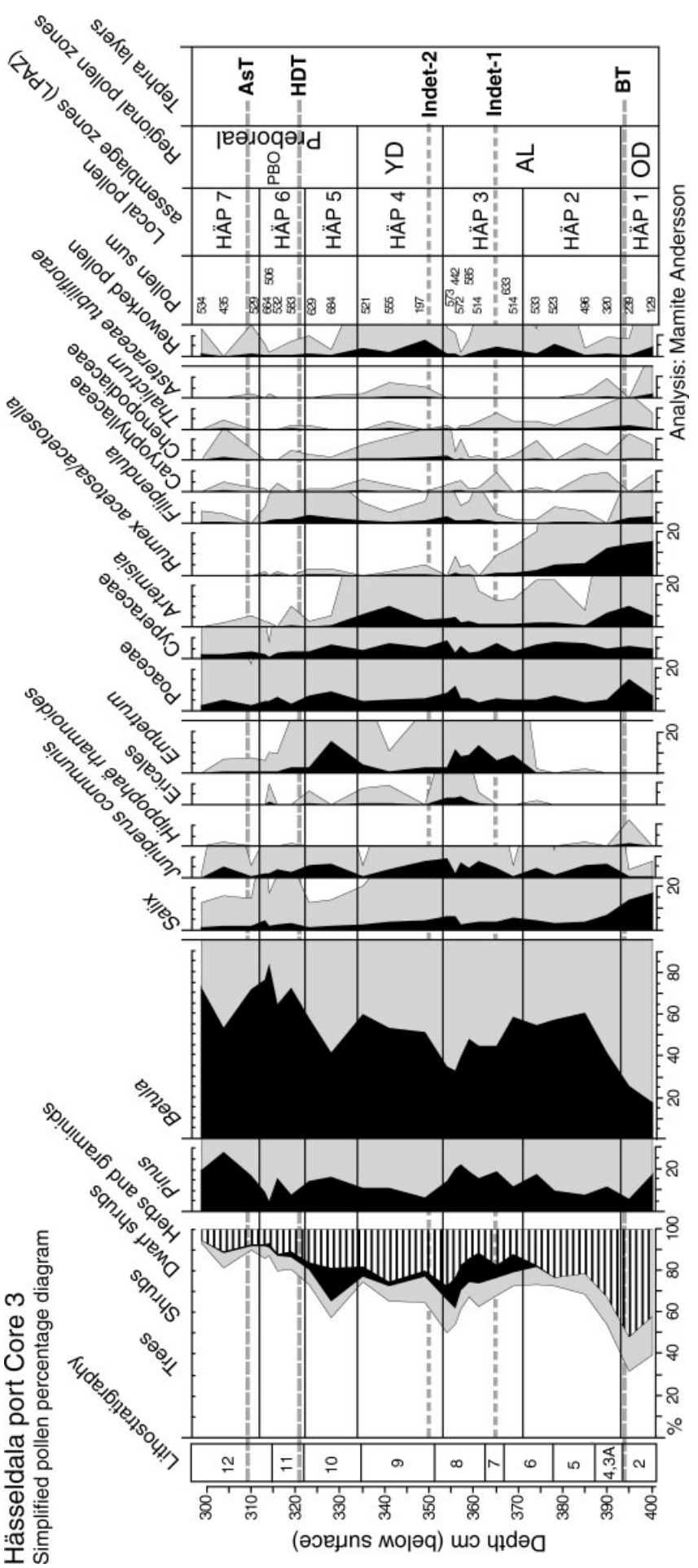

Figure 3 Summary pollen percentage diagram for core 3 at Hässeldala port (modified after Davies *et al.*, 2004b) and correlation of the local pollen assemblage zones to the regional pollen stratigraphy of Björck (1979, 1984) for southernmost Sweden. The grey area represents × 10 exaggeration. Reworked taxa include *Corylus, Ulmus, Alnus, Quercus, Populus, Carpinus*. Pollen sum = terrestrial pollen. OD = Older Dryas, AL = Allerød, YD = Younger Dryas, PBO = Preboreal Oscillation, BT = Borrobol Tephra, Indet. = unidentified tephra, HDT = Hässeldalen Tephra, AsT = 10-ka Askja Tephra. For details on the lithostratigraphic units 2–12 see Fig. 2

All three cores show a gradual increase in TC content in the basal sandy, silty and clayey sediments (units 1, 2, 3B), a more marked increase at the transition to the clay gyttja in unit 3A, fluctuating values in the gyttja layers of units 4 and 5 and a slight decrease in unit 6. Subsequent to the distinct peak in unit 7, TC declines and has fairly low and stable values in unit 8. The renewed, rapid increase in TC during unit 9 is followed by high, but fluctuating values in units 10–12 (Fig. 2). These fluctuations include a distinct TC minima in sediment unit 11 at 244–241 cm (core 1), 250–248 cm (core 2) and 316–313 cm (core 3), respectively. TC is generally assumed as a measure of lake productivity and intervals with lower/higher values may thus correspond to periods with lower/higher lake productivity.

Geochemical identification of the tephra horizons was undertaken on samples from core 1 and the results are reported in Davies *et al.* (2003). Only the peak shard concentrations were determined in cores 2 and 3. The BT occurs at a depth of 303 cm in core 1, at 302 cm in core 2 and at 394 cm in core 3, just below the transition between sediment units 2 and 3B (Fig. 2). The two unidentified tephra layers were only detected in core 1 at depths of 278 cm (sediment unit 6) and 266 cm (sediment unit 8) respectively. Low shard concentration (Davies *et al.*, 2003) and the uneven distribution of tephra horizons in general, may explain why these cryptotephras were not found in cores 2 and 3. The HDT, found in core 1 at 247 cm and in core 3 at 321–322 cm, lies on the slope of the increasing TC curve, at the transition between sediment units 9 and 10. The youngest tephra of the Hässeldala sequence, the AsT occurs at a depth of 238 cm in core 1 and at 308–310 cm in core 3.

The pollen stratigraphy, which was established on core 3 (Fig. 3), covers the sediments between 400 and 300 cm depth and thus extends from the middle part of sediment unit 2 to sediment unit 12. The LPAZs HÄP 1–7 are described in Table 1 and correlated to the regional pollen stratigraphy for southeast Sweden (Björck, 1979; Björck and Möller, 1987; Björck *et al.*, 1996). The correlation shows that the analysed part of the sequence encompasses the regional Older Dryas, Allerød, Younger Dryas and Preboreal pollen zones. A distinct characteristic of the Older Dryas pollen zone in southeast Sweden is the first occurrence of *Hippophaë* pollen (HÄP 1), which is followed by an increase in *Juniperus* (Allerød I) and *Empetrum* pollen percentages (Allerød II) (HÄP 2, 3) (Björck, 1979, 1984) (Fig. 3). The distinct increase in *Artemisia* pollen values along with a decline in *Empetrum* (HÄP 4), can be observed in all south Swedish pollen diagrams covering this time interval and marks the Younger Dryas pollen zone (Berglund *et al.*, 1994; Björck *et al.*, 1996). The renewed rise in *Empetrum* pollen percentages and the coincident decline in *Artemisia* pollen values (LPAZ HÄP 5) has formerly been attributed to the upper part of the Younger Dryas pollen zone and was named YD III (Björck, 1979; Björck and Möller, 1987) or 'Younger Dryas–Preboreal transition zone', but is now assigned to the beginning of the Preboreal pollen zone (Björck *et al.*, 1996). High pollen values for *Betula* and *Pinus* and a decrease of non-arboreal pollen (LPAZ HÄP 6, 7) are characteristic of the middle and upper part of the Preboreal pollen zone. In addition, the distinct increase in *Salix* pollen values at 314 cm in HÄP 6, which coincides with a decline in *Pinus* pollen percentages (Fig. 3), can be related to the Preboreal Oscillation (PBO) as defined by Björck *et al.* (1997) for southern Sweden.

The LPAZs established on core 3 can be tentatively transferred to cores 1 and 2 through a correlation of the three TC curves (Figs 2 and 4). This correlation indicates that a minor increase in TC in all three cores and thus in lake productivity occurred before and during the Older Dryas pollen zone. Lake productivity increased during Allerød I, but declined again shortly in Allerød II. This decline could possibly be associated with the so-called 'Gerzensee Oscillation' (Lotter *et al.*, 1992; Andresen *et al.*, 2000). The distinct peak in TC visible in all three cores during the upper part of HÄP 3 is characteristic for many lake sediment sequences in south Sweden (Berglund *et al.*, 1994). It may reflect increased lake productivity, but could also be due to increased inwash of terrestrial plant material. During the regional Younger Dryas pollen zone inferred lake productivity remained low, but increased again rapidly during the early Preboreal (Fig. 4). A phase with distinctly lower TC values is visible in HÄP 6 (244–241 cm in core 1; 250–248 cm in core 2; 316–313 cm in core 3) and coincides

Table 1 Correlation of the local pollen assemblage zones (LPAZ) at Hässeldala port, core 3 with the regional pollen stratigraphy for Blekinge, southeast Sweden (Björck, 1979; Björck and Möller, 1984). The original YD III pollen zone is now placed within the Preboreal pollen zone (Björck *et al.*, 1996). PBO = Preboreal Oscillation according to Björck *et al.* (1997)

LPAZ	Depth (cm)	Description	Regional pollen zone
HÄP 7	312–300	*Pinus–Juniperus* zone Marked increase of *Pinus* and high values of *Betula*	Preboreal
HÄP 6	322–312	*Betula* zone Low herb and shrub pollen values, dominance of *Betula;* distinct increase of *Salix* and decrease of *Pinus* in upper part of the zone	Preboreal, incl. PBO
HÄP 5	334–322	*Empetrum–Juniperus*–Poaceae zone Increase in *Pinus*, distinct *Empetrum* peak, increase *Juniperus*, decrease of *Artemisia*	Younger Dryas/YD III Preboreal
HÄP 4	355–334	*Artemisia–Betula–Juniperus* zone Increase in herb and shrub pollen, high *Betula*, but low *Pinus*. Distinct decrease in *Empetrum* and marked increase in *Artemisia*	Younger Dryas/YD I, II
HÄP 3	371–355	*Empetrum–Pinus–Betula* zone High *Betula* and *Pinus* and low herb pollen values, distinct increase in *Empetrum*	Allerød/AL II
HÄP 2	393–371	*Betula–Rumex* zone Herb and grass pollen values decrease and *Juniperus* and tree pollen values increase	Allerød/AL I
HÄP1	400–393	*Rumex–Salix–Artemisia*–Poaceae zone High frequencies of herb, graminid, shrub pollen, low values of tree pollen; first occurrence of *Hippophaë*	Older Dryas

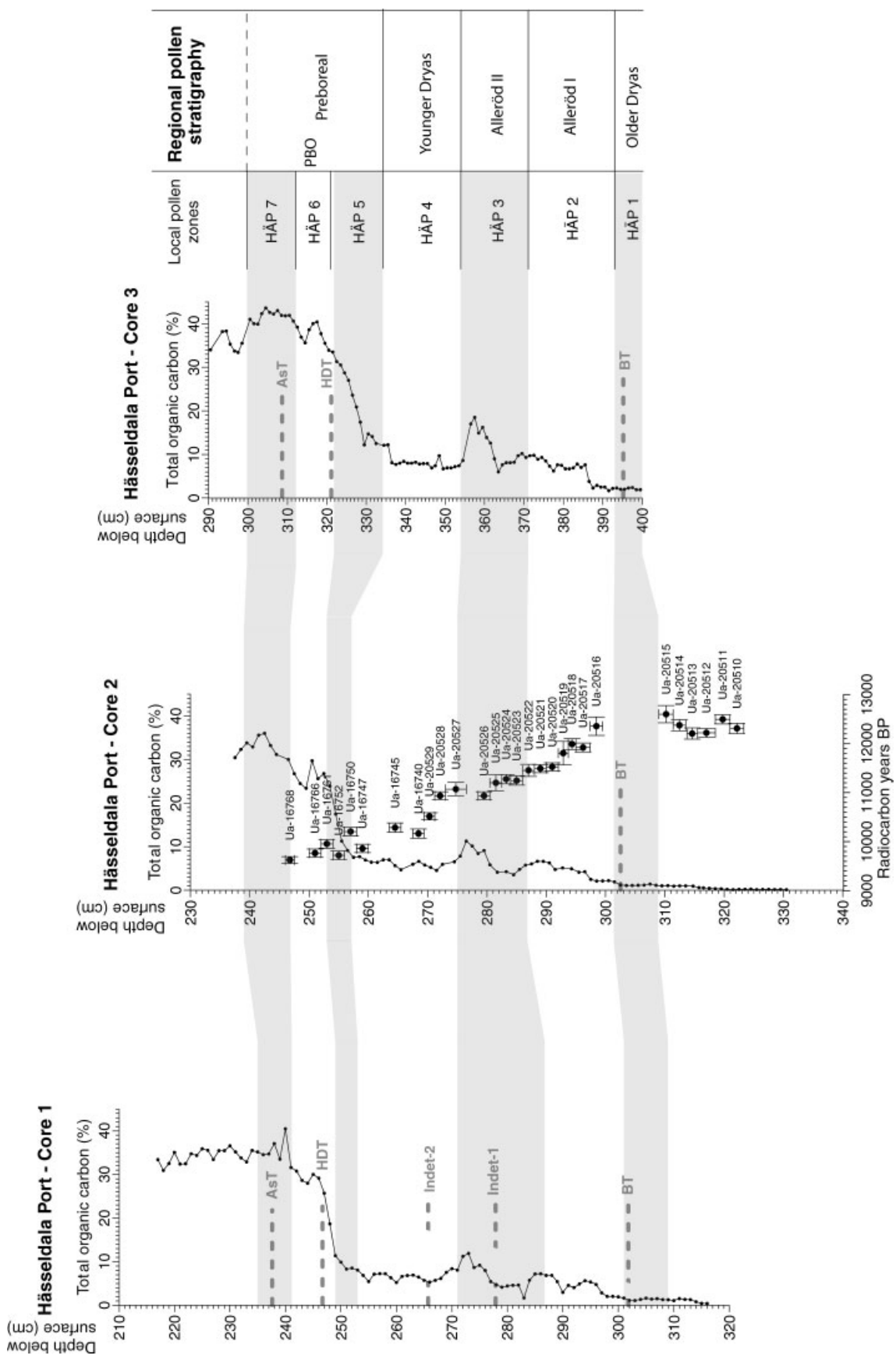

Figure 4 Correlation of the local pollen assemblage zones (LPAZ) HÄP 1–7 in core 3 to corresponding levels in cores 1 and 2, based on wiggle-matching of the TC curves (see Fig. 2). Details on the ^{14}C measurements from core 2 are shown in Table 2. The cryptotephra layers found in the three sequences are indicated by dashed lines. BT = Borrobol Tephra, HDT = Hässeldalen Tephra, AsT = 10-ka Askja Tephra, Indet = unidentified tephra

with the change in pollen spectra discussed above and attributed to the PBO.

The correlation between cores 1–3 (Fig. 4) shows that the BT falls at the very end of the Older Dryas pollen zone as discussed previously by Davies *et al.* (2004b). The older of the two unidentified cryptotephras (Indet-1), discovered in core 1, occurs in the Allerød II pollen zone, during an interval with lower TC values, which may correspond to the Gerzensee Oscillation. The second unidentified tephra (Indet-2) is assigned to the early part of the Younger Dryas pollen zone and the two youngest tephras (HDT, AsT) to the Preboreal pollen zone. The HDT, which has been found in cores 1 and 3, occurs shortly before the PBO and the AsT falls shortly after the PBO.

Age models

The radiocarbon ages obtained earlier on core 2, between 323 and 270 cm depth (Davies *et al.*, 2004b) are here supplemented by eight new measurements between 270 and 246 cm. A total of 28 radiocarbon measurements are thus available for the entire sequence, ranging from ca. 12 600 to ca. 9600 ^{14}C yr BP (Table 2). Plotted against depth, the ^{14}C dates follow the general trend of Lateglacial and early Holocene ^{14}C variations with several short and longer ^{14}C plateaux (Reimer *et al.*, 2004) (Fig. 4). The age–depth curve, however, indicates that some of the measurements may have yielded ages that are too old (Ua-20511, 20514, 20515, 20516) or too young (Ua-16740, 16747, 16752). Indeed, samples Ua-20514, 20515 and 20516 contained heavily corroded leaves and leaf fragments (Table 2), which are most likely reworked from older sediments. Samples that appear to have too young ages may be related to small sample size which increases the possibility of contamination by recent material (Wohlfarth *et al.*, 1998).

In model A the ^{14}C measurements were wiggle-matched to the IntCal04 calibration curve (Reimer *et al.*, 2004) in the program Bpeat (Blaauw and Christen, 2005), by assuming linear accumulation of the entire sequence and excluding lithostratigraphic information (Fig. 5(a) and (d)). Prior assumptions were that (i) accumulation rates range between ca. 20 and 80 yr cm^{-1}, but that lower and higher accumulation rates are possible, albeit less likely; and (ii) prior outlier probabilities were 50% for those measurements which included corroded plant material (Table 2), and 5% for other measurements. Model results show that not all ^{14}C dates (1 s.d. error bars) overlap with the IntCal04 calibration curve (Fig. 5(a)) and that the fit F is 83.84% (see Blaauw and Christen, 2005). In particular, ^{14}C dates Ua-16752, Ua-16747, Ua-20528, Ua-20527, Ua-20520, Ua-20516, Ua-20512 and Ua-20510 obtained high posterior probabilities of being outliers, while of these dates only Ua-20520 and Ua-20516 contained corroded plant material (Table 2). Other dates with corroded plant material (Ua-20514 and Ua-20515) fall on the calibration curve. The estimated accumulation rate for the entire sequence was ca. 53 yr cm^{-1}.

In model B the sequence was subdivided into three sections, assuming linear accumulation within each section, and wiggle-matched to IntCal04 using the program Bpeat (Fig. 5(b) and (e)). Division levels were not fixed to certain depths, but were estimated automatically by the software. In addition, this match was solely based on the ^{14}C dates and prior information as in

Table 2 AMS ^{14}C measurements along core 2 from Hässeldala port

Sample ID	Laboratory no. Ua-	Depth (cm)	Dated material	^{14}C yr BP $\pm 1\sigma$
H4	20510	322.15 ± 1.15	*Betula nana* (L), *Salix polaris* (L), *Salix* sp. (W)	12 310 ± 105
H5	20511	319.75 ± 1.25	*Betula nana* (L), *Salix polaris* (L), *Salix* sp. (L)	12 495 ± 95
H6	20512	317 ± 1.5	*Betula nana* (L), *Salix polaris* (L), *Salix* sp. (L)	12 220 ± 90
H7	20513	314.6 ± 0.9	*Betula nana* (L), *Salix polaris* (L), *Salix* sp. (L)	12 205 ± 115
H8	20514	312.45 ± 1.05	*Betula nana* (L), *Salix polaris* (L), *Salix* sp. (L)*	12 375 ± 115
H9	20515	310.2 ± 1.2	*Betula nana* (L), *Salix polaris* (L), *Salix* sp. (L), *Dryas octopetala* (L)*	12 600 ± 175
H14	20516	298.45 ± 1.05	*Betula nana* (S, C), *Dryas octopetala* (L), indet. (L)*	12 355 ± 190
H15	20517	296.2 ± 0.65	*Betula nana* (L, S, C, W), *Dryas octopetala* (L)	11 920 ± 90
H16	20518	294.35 ± 0.65	*Betula nana* (L, S, C, W), *Dryas octopetala* (L)	11 990 ± 110
H17	20519	292.85 ± 0.85	*Betula nana* (L, S, C)*	11 805 ± 240
H18	20520	291 ± 1	*Betula nana* (L, S, C, W)*	11 525 ± 85
H19	20521	289 ± 1	indet. (W)	11 490 ± 85
H20	20522	287 ± 1	*Betula nana* (L, C)	11 455 ± 125
H21a	20523	285 ± 1	*Betula nana* (L, S, C), indet. (W)	11 245 ± 95
H22	20524	283.25 ± 0.75	*Betula nana* (L, S, C), indet. (W)	11 275 ± 95
H23	20525	281.5 ± 1	*Betula nana* (L, S, C)	11 200 ± 165
H24	20526	279.5 ± 1	*Betula nana* (L, S, C), indet. (W)	10 935 ± 80
H26 + 27	20527	274.75 ± 1.75	*Betula nana* (L, S, C), indet. (W)	11 070 ± 135
H28	20528	272.1 ± 0.9	*Betula nana* (L, S, C), indet. (W)	10 935 ± 80
H29	20529	270.3 ± 0.9	*Betula nana* (L, S, C), indet. (W)	10 515 ± 75
H30	16740	268.45 ± 0.95	*Betula nana* (L)	10 165 ± 95
H32	16745	265.5 ± 1	*Betula nana* (L, C), indet. (W)	10 285 ± 95
H35	16747	259 ± 1	*Betula nana* (L), indet. (W)	9860 ± 85
H36a	16750	257 ± 1	*Betula nana* (L); indet. (W), charcoal	10 205 ± 85
H37	16752	255 ± 1	*Betula nana* (L), *Betula pubescens* (S), *Pinus sylvestris* (N)	9720 ± 90
H38	16761	253 ± 1	*Betula nana* (L), indet. (W)	9955 ± 90
H39	16766	251 ± 1	*Betula nana* (L), *Pinus sylvestris* (N)	9765 ± 85
H41a	16768	246.75 ± 0.75	*Pinus sylvestris* (N)	9625 ± 70

L = leaves and leaf fragments; W = wood fragments; S = seeds; C = catkin scales; N = needles; * = heavily corroded plant remains.

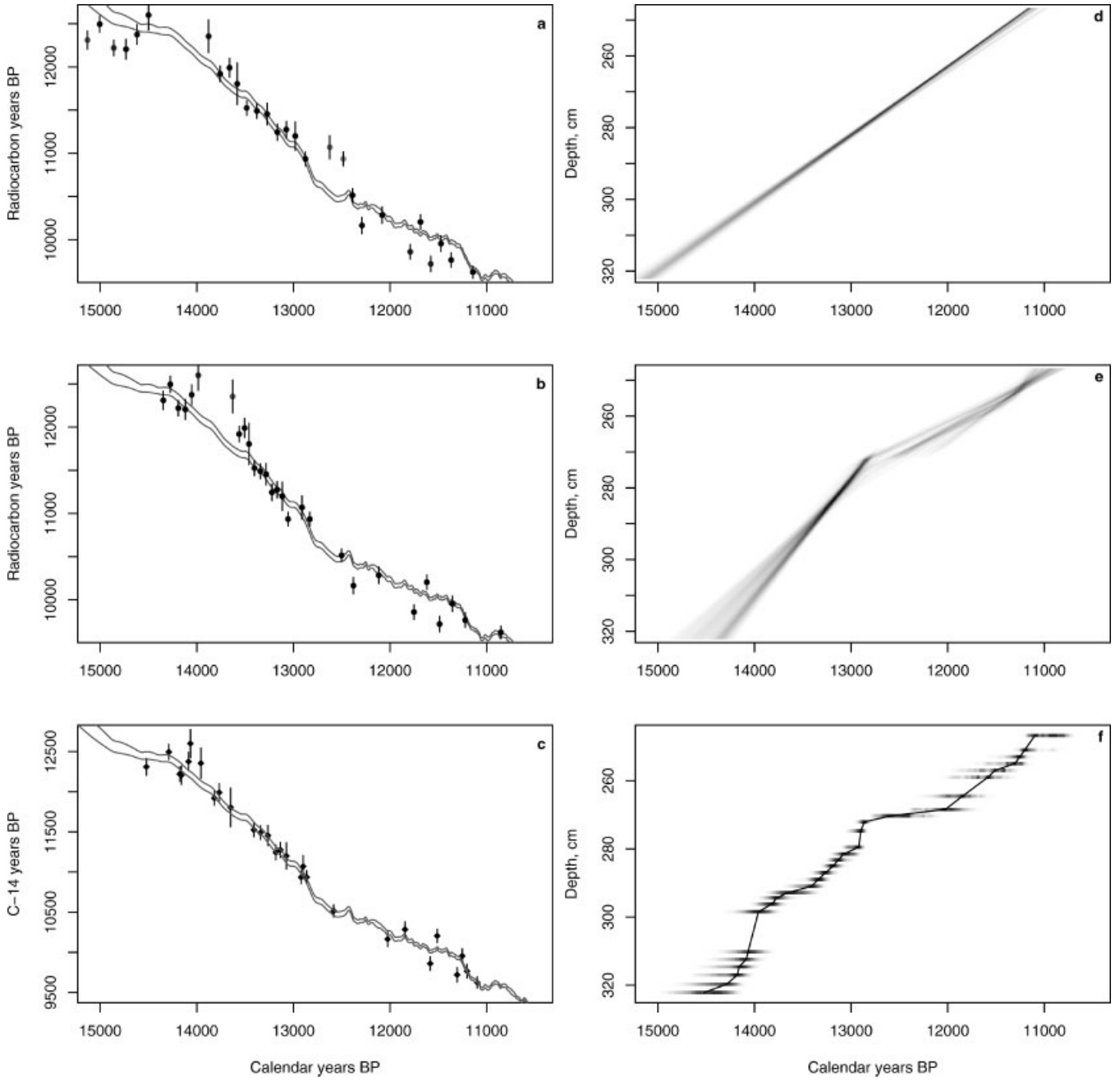

Figure 5 (a)–(c) Placement of the ^{14}C dates on the IntCal04 calibration curve (Reimer *et al.*, 2004), using the programme Bpeat (Blaauw and Christen, 2005), (a) Model A, (b) Model B, (c) Model C. Calendar-year ages were given to the dated levels as proposed by the maximum posterior densities of their chronological ordering-constrained calibrated ranges. (d)–(f) Corresponding age model, where the grey scales indicate the likelihood of calendar ages for the dated levels. Darker colours indicate more likely calendar ages. The bold curve connects the highest posterior densities of the neighbouring levels, (d) Model A, (e) Model B, (f) Model C

model A, but included the following additional prior information: (i) very low dependency of the accumulation rate between the sections; (ii) hiatus lengths of up to ca. 100 yr are possible, but shorter lengths are much more likely. This match resulted in a better fit than model A ($F = 92.71\%$; Blaauw and Christen, 2005) (Fig. 5(b)), but gave the following outliers: Ua-16752, Ua-16740, Ua-20516 and Ua-20514. Only the last two samples contained corroded plant material and were thus suspected of being too old beforehand.

For model C, which was computed in Bcal (Buck *et al.*, 1999), the entire sequence was matched against the IntCal04 calibration curve, assuming chronological ordering (Fig. 5(c) and (f)). Samples Ua-16747, Ua-16750, Ua-20515 and Ua-20516 did not match the calibration curve within their 1 s.d. error bars, but only samples Ua-20515 and Ua-20516 had been assumed to be too old beforehand (Table 2).

The Bayesian modelling techniques described above use thousands to millions of so-called Markov chain Monte Carlo (MCMC) iterations to derive estimates of the parameters involved in an age model. Besides estimating calendar ages for the ^{14}C dated levels (i.e. the pollen zone boundaries HÄP 2/3, HÄP 3/4, HÄP 4/5 and HÄP 5/6), these methods can also be used to estimate the ages of non-^{14}C dated levels (i.e. pollen zone boundaries HÄP 1/2 and HÄP 6/7, and tephras BT and HDT). For models A and B, calendar age estimates for non-dated levels within the ^{14}C sequence were straightforward as these models are based on piecewise, linear accumulation. For model C, calendar ages for the non-dated levels were estimated through providing relative information, i.e. Bcal was for example informed that the BT horizon is older than date Ua-20516, but younger than Ua-20515. The tephra horizon AsT, however, is assumed to be located 2–3 cm above the ^{14}C dated

part of core 2 (Fig. 4), and therefore needed an extrapolation to obtain an age estimate. For models A and B we simply extrapolated the MCMC-derived age-estimate to the required depth of AsT. We are aware that extrapolation is dangerous, and that the corresponding age estimate for AsT should be considered with caution. For model C a sensible upper age limit to constrain the age of AsT is missing. Therefore, its calendar age distribution could not be calculated for model C.

Discussion

Davies *et al.* (2004b) presented and discussed three different age models for the BT at Hässeldala port, based on visual wiggle-matching of the ^{14}C dates to the Cariaco Basin data set (Hughen *et al.*, 1998, 2000) and on a Bayesian probability approach using the Cariaco (Hughen *et al.*, 1998, 2000) and Lake Suigetsu (Kitagawa and van der Plicht, 2000) time series. These age models included fewer ^{14}C dates than the age models presented here and estimated the age of the BT to ca. 13 900 Cariaco varve years BP (visual match) and 14 450–13 800 and 14 331–13 667 cal. yr BP, respectively. The Bayesian approach adopted here includes wiggle-matching of a total of 28 ^{14}C dates to the new IntCal04 calibration curve (Reimer *et al.*, 2004) under the assumptions of linear accumulation (Model A), linear accumulation between sections (Model B) and chronological ordering of ^{14}C dates (Model C).

Although the ^{14}C wiggle-match in Model A gives a rather nice fit to the radiocarbon calibration curve (Fig. 5(a)), the fit F of 83.83% is clearly below the >90% fit suggested by Blaauw and Christen (2005). ^{14}C dates from the lower end of the sequence and between 12 500 and 11 000 cal. yr BP appear to be outliers. The grey-scale graph in Fig. 5(d) displays a very narrow uncertainty range, but considering that the age model only uses one single section to fit the dates to the calibration curve, this model might give an 'illusionary precise picture', as it might have forced dates to certain calendar ages. In Model B (Fig. 5(b)), which has a fit F of 93.45%, two dates around 13 500 cal. yr BP and dates around 12 500 and 11 500 cal. yr BP are the only outliers. As can be seen in Fig. 5(e), this model has rather large uncertainty ranges, which can be explained by the fact that it subdivided the sequence into three sections (with variable division depths), which in turn resulted in many different possible solutions. Model C is only constrained by chronological ordering (Fig. 5(c) and (f)) and results in a nice match of most ^{14}C dates. Outliers in this model are related to those ^{14}C measurements which were beforehand suspected of being too old.

The comparison between the three models (Fig. 5(a)–(f) shows, that model A gives narrow confidence intervals (Fig. 5(d), Table 3), but that it has some clear disadvantages (low fit F, unexpected outliers, assumption of linear accumulation of the entire core) over models B and C. Also the assumption of linear accumulation over long periods (e.g. an entire sequence), is not applicable for lake sediments, where sediment composition and sedimentation rates change rapidly and shorter hiatuses may be frequent. Models B and C show partly similar results but model C uses fewer assumptions than model B and does not allow extrapolation beyond the dated range. The confidence intervals for pollen zone boundaries and tephra horizons (Figs 6 and 7, Table 3) provided by model B are, with a few exceptions, narrower than those of model C. Thus, given the clear limitations of model A, we focus in the following discussion only on the calendar-year estimates given by models B and C.

The boundary between the Older Dryas/Allerød regional pollen zone (HÄP 1/HÄP 2) is estimated to 13 934–13 666 cal. yr BP (model B) or 14 226–13 808 cal. yr BP (model C) (Table 3), which corresponds approximately in time to the transition from GI-1d to GI-1c in the GRIP event stratigraphy

Table 3 Calendar-age estimates (95% confidence intervals) for tephra horizons, local and regional pollen zone boundaries at Hässeldala port derived from age models A and B (see also Figs 4 and 5(a)–(f). BT = Borrobol tephra, Indet = unidentified tephra, HDT = Hässeldala Tephra, AsT = 10-ka Askja Tephra, HÄP = local pollen zones, OD = Older Dryas, AL = Allerød, YD = Younger Dryas, PB = Preboreal

	Model A cal. yr BP	Model B cal. yr BP	Model C cal. yr BP
Tephra horizons			
BT	14 226 – 14 105	14 013 – 13 713	14 259 – 13 833
	14 165 ± 60	13 836 ± 150	14 046 ± 213
Indet-1	13 063 – 12 965	13 239 – 13 049	13 207 – 12 964
	13 014 ± 49	13 144 ± 95	13 085 ± 121
Indet-2	12 461 – 12 335	12 860 – 12 196	12 906 – 12 375
	12 398 ± 49	12 528 ± 332	12 640 ± 265
HDT	11 565 – 11 299	11 543 – 11 232	11 596 – 11 164
	11 432 ± 133	11 387 ± 155	11 380 ± 216
AsT	11 070 – 10 750	11 050 – 10 570	—
	10 910 ± 160	10 810 ± 240	—
Local (and regional) pollen-zone boundaries			
End of HÄP 1 (OD/AL)	14 113 – 13 917	13 934 – 13 666	14 226 – 13 808
	14 015 ± 98	13 800 ± 134	14 017 ± 209
HÄP 2/HÄP 3	13 315 – 13 203	13 397 – 13 239	13 391 – 13 156
	13 259 ± 56	13 318 ± 79	13 273 ± 117
HÄP 3/HÄP 4 (AL/YD)	12 671 – 12 559	13 065 – 12 623	13 021 – 12 841
	12 615 ± 56	12 844 ± 221	12 931 ± 90
HÄP 4/HÄP 5 (YD/PB)	11 733 – 11 495	11 722 – 11 406	11 876 – 11 293
	11 614 ± 119	11 564 ± 158	11 585 ± 292
HÄP 5/HÄP 6	11 537–11 271	11 422 – 11 216	11 547 – 11 128
	11 404 ± 133	11 319 ± 103	11 337 ± 209
HÄP 6/HÄP 7	11 229 – 10 907	11 137 – 10 805	11 235 – 10 815
	11 068 ± 161	10 971 ± 166	11 025 ± 210

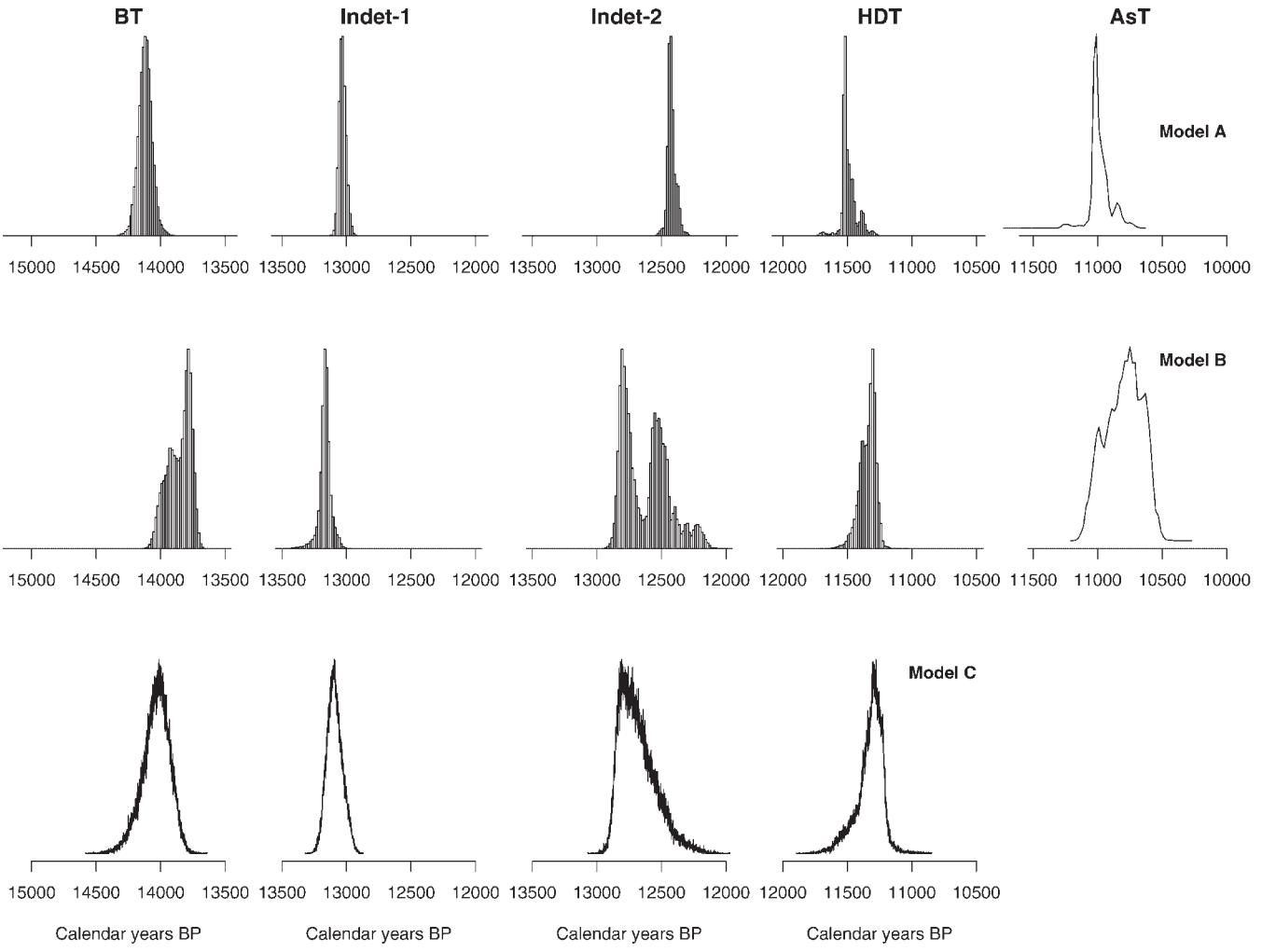

Figure 6 Age estimates for the different tephra layers according to age models A (top panel), B (middle panel) and C (lower panel); the black line connects the maxima of the constrained calibrated ranges. BT = Borrobol Tephra, Indet. = inidentified tephra, HDT = Hässeldala Tephra, AsT = 10-ka Askja Tephra

(Björck *et al.*, 1998; Walker *et al.*, 1999). The BT occurs at the very end of the Older Dryas pollen zone and is given an age estimate of 14 013–13 713 cal. yr BP (model B) or 14 259–13 833 cal. yr BP (model C) (Fig. 6, Table 3). These estimates provide improved constraints on the age limits of the BT as compared to Davies *et al.* (2004b) and confirm the earlier hypothesis that the BT found at Hässeldala port is considerably younger than indicated from other European sequences (Lowe *et al.*, 1999; Eiriksson *et al.*, 2000). It seems to correspond in time with a 'Borrobol-like' cryptotephra, recently discovered in northwest Scotland and attributed to the early Allerød (Ranner *et al.*, 2005).

The lower of the two unidentified tephras (Indet-1) falls within the regional Allerød II pollen zone (HÄP 3), just before the rise in TC content seen in all three sequences (Fig. 4) and is estimated to 13 239–13 049 cal. yr BP (model B) or 13 207–12 964 cal. yr BP (model C) (Fig. 6, Table 3). The litho- and pollen stratigraphic position of the tephra horizon could indicate that it is a correlative of the Laacher See Tephra, which has been traced in, for example, Switzerland at the end of the Gerzensee Oscillation (Lotter *et al.*, 1992, 1995).

The transition between the regional Allerød II/Younger Dryas pollen zone (HÄP 3/HÄP 4) has an age estimate of 13 065–12 623 cal. yr BP (model B) or 13 021–12 841 cal. yr BP (model C), which is close to the age for the boundary between GI-1a and GS-1 (Björck *et al.*, 1998; Walker *et al.*, 1999). The second unidentified tephra (Indet-2) correlates to the lower part of the regional Younger Dryas pollen zone and is estimated to 12 860–12 196 cal. yr BP (model B) or 12 906–12 375 cal. yr BP (model C) (Table 3). This age assignment makes it significantly older than the accepted age of the Vedde Ash (10 300 ^{14}C yr BP or 12 000 GRIP ice core yr BP; Grönvold *et al.*, 1995; Birks *et al.*, 1996; Wastegård *et al.*, 1998). Without any geochemical information it is difficult to determine the origin of this tephra, although a tephra of early Younger Dryas age and older than the Vedde Ash has been identified in Sluggan Bog (Lowe *et al.*, 2004).

The regional Younger Dryas/Preboreal (HÄP 4/HÄP 5) pollen zone boundary has an age estimate of 11 722–11 406 cal. yr BP (model B) or 11 876–11 293 cal. yr BP (model C), which is close in time to the transition between GS-1 and the Holocene (Björck *et al.*, 1998; Walker *et al.*, 1999). The two youngest tephras (HDT, AsT) bracket the PBO and are recorded just below and above this climatic shift (Figs 3 and 4). The position of the HDT and AsT, before and after the PBO makes them potentially useful for time-synchronous correlations in various parts of Europe. The HDT is estimated to 11 543–11 232 cal. yr BP (model B) or 11 596–11 164 cal. yr BP (model C) and the AsT to 11 050–10 570 cal. yr BP (model B) (Table 3).

Constructing robust chronologies for Lateglacial lake sediment sequences such as Hässeldala port by the application of high-resolution ^{14}C dating, tephra horizons and Bayesian probability methods is evidently not a straightforward procedure. The errors associated with radiocarbon dating (Björck and

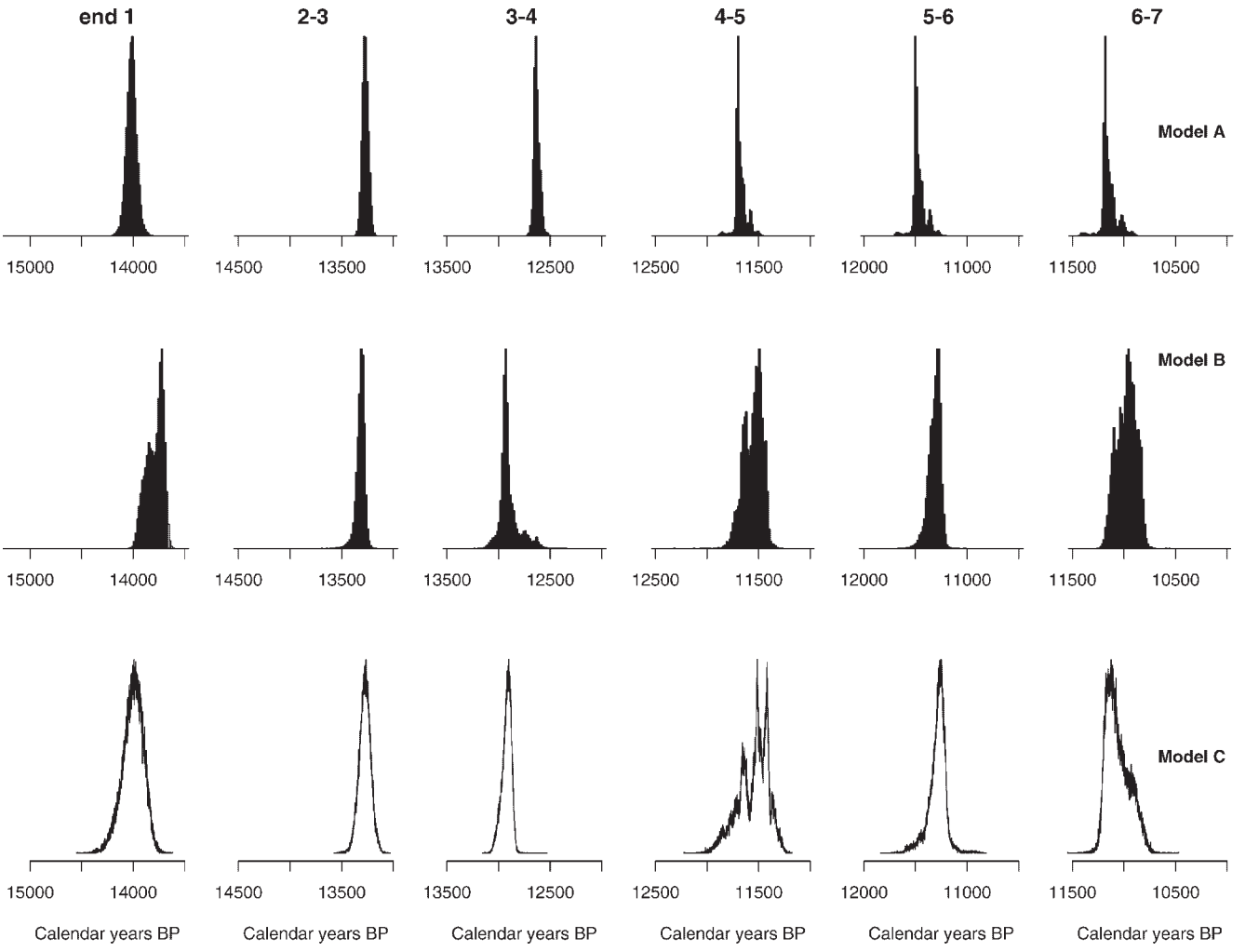

Figure 7 Age estimates for the local pollen zones according to models A (top panel), B (middle panel) and C (lower panel). See Fig. 3 for the pollen diagram

Wohlfarth, 2001) and calibration procedures are further confounded by uncertain sedimentation rates within lacustrine environments that may vary considerably due to topographic, climatic and environmental conditions. In addition, short hiatuses are often very difficult to detect and thus, in the absence of an annually laminated sequence, it is impossible to determine the sedimentation rates and the degree of variability with any degree of confidence during the Lateglacial period. Taking account of these limitations and including these as prior assumptions are critical for the establishment of valid and 'realistic' age models. This information is not always easy to incorporate into the exercise of constructing age–depth models and is as such often overlooked. The Bayesian probability methods outlined in this paper, however, in which these prior assumptions are incorporated represent the best available approach for the derivation of a robust high-resolution age–depth model for the Lateglacial period. Even so, this exercise has emphasised that it is difficult to solely use one model as limitations are recognised in all approaches. For instance, Model B might place too much confidence on the assumption of linear accumulation, an assumption which is probably unrealistic since rapid and large environmental changes occurred during this time period. On the other hand, the fact that ^{14}C ages could be imprecise would warrant against using model C, as this model perhaps places too much confidence on the dates being correct, and correspondingly infers changes in accumulation rate between each dated level. With our current level of information we cannot state which of the two models provides the best age estimates. Accordingly the age ranges provided by models B and C are much larger, thus creating difficulties for precise correlations to other archives to determine leads/lags. Nevertheless, this exercise provides the best constrained, statistically reliable age estimates for the five tephra layers and the local pollen zones. Our results further support the position of the BT as found in southern Sweden at the end of the Older Dryas pollen zone and provide the first age estimates and pollen stratigraphic position for the 10-ka Askja and Hässeldalen tephras. This framework can be used for tracing these tephras in other palaeoclimatic sequences. Furthermore, our study highlights the dangers of solely accepting one age model for the derivation of a robust, statistically constrained chronology that can be compared to other palaeoarchives. Different age models will result in different age estimates and depending on the model that was chosen, published age estimates will probably be incompatible between sequences. A possible solution to this problem could be to radiocarbon-date a sequence with ultra-high resolution, to measure each radiocarbon sample long enough to increase its precision and to explore a number of different age–depth models so that various scenarios and factors can be incorporated into each model and evaluated individually.

In addition, tephra horizons can be employed as isochronous marker horizons on a continent-wide scale (Turney *et al.*, 2004) which can preclude some of the uncertainties associated with the construction of ^{14}C age–depth models. Tephrochronology, however, is also subject to uncertainties as shown here in the

case of the BT tephra. There is therefore, clearly a need for the application of a more diagnostic geochemical technique, for example, trace element analysis by Laser Ablation–Inductively Coupled Plasma Mass Spectrometry (Pearce *et al.*, 2004) as well as deriving independent age estimates for these tephra horizons by their identification within the Greenland ice cores or annually laminated sequences. These approaches may then provide key time-synchronous correlations between different palaeoclimatic archives (Davies *et al.*, 2004a; Mortensen *et al.*, 2005). However, as the search for tephra and more specificially cryptotephra horizons is still at an early stage within such records, it is not currently possible to trace the same tephra horizons as tie points in all geological sequences due to variable dispersal patterns and taphonomic processes operating at a local scale. Consequently, radiocarbon dating is still an integral part of providing age estimates for tephra horizons and for constructing age–depth models during the Lateglacial period. Although the age ranges for the tephra horizons outlined here are large, the Bayesian probability methods followed provide the best constrained and statistically significant age estimates that are currently available given the uncertainties associated with constructing age–depth models during the Lateglacial period.

Acknowledgements We thank Ann Karlsson and Nagham Mahmoud for measuring the TC on cores 1–3, Sven Karlsson for help with the TILIA programme and Svante Björck for discussions. We appreciated the helpful review comments by John Pilcher.

References

Andresen CS, Björck S, Bennike O, Heinemeier J, Kromer B. 2000. What do ^{14}C changes across the Gerzensee oscillation/GI-1b event imply for deglacial oscillations? *Journal of Quaternary Science* **15**: 203–214.

Berglund BE, Ralska-Jasiewiczowa M. 1986. Pollen analysis and pollen diagrams. In *Handbook of Holocene Palaeoecology and Palaeohydrology*, Berglund BE (ed.). Wiley: Chichester; 455–484.

Berglund BE, Bergsten H, Björck S, Kolstrup E, Lemdahl G, Norberg K. 1994. Late Weichselian environmental change in southern Sweden and Denmark. *Journal of Quaternary Science* **9**: 127–132.

Birks HH, Gulliksen S, Haflidason H, Mangerud J, Possnert G. 1996. New radiocarbon dates for the Vedde Ash and the Saksunarvatn Ash from western Norway. *Quaternary Research* **45**: 119–127.

Björck S. 1979. *Weichselian stratigraphy of Blekinge, SE Sweden, and water level changes in the Baltic Ice Lake*. LUNDQUA Thesis, no. 7.

Björck S. 1984. Bio- and chronostratigraphic significance of the Older Dryas Chronozone—on the basis of new radiocarbon dates. *Geologiska Föreningen i Stockholm Förhandlingar* **106**: 81–91.

Björck S, Möller P. 1987. Late Weichselian environmental history in southeastern Sweden during the deglaciation of the Scandinavian ice sheet. *Quaternary Research* **28**: 1–37.

Björck S, Wohlfarth B. 2001. ^{14}C chronostratigraphic techniques in paleolimnology. In *Tracking Evironmental Changes Using Lake Sediments*, Last WM, Smol JP (eds). Kluwer: Dordrecht; 205–245.

Björck S, Kromer B, Johnsen S, Bennike O, Hammarlund D, Lemdahl G, Possnert G, Rasmussen TL, Wohlfarth B, Hammer CU, Spurk M. 1996. Synchronised terrestrial–atmospheric deglacial records around the North Atlantic. *Science* **274**: 1155–1160.

Björck S, Rundgren M, Ingolfsson O, Funder S. 1997. The Preboreal oscillation around the Nordic Seas: terrestrial and lacustrine responses. *Journal of Quaternary Science* **12**: 455–466.

Björck S, Walker MJC, Cwynar LC, Johnsen S, Knudsen KL, Lowe JJ, Wohlfarth B, INTIMATE members. 1998. An event stratigraphy for the Last Termination in the North Atlantic region based on the Greenland ice-core record: a proposal by the INTIMATE group. *Journal of Quaternary Science* **13**: 283–292.

Björck S, Muscheler R, Kromer B, Andresen CS, Heinemeier J, Johnsen SJ, Conley D, Koc N, Spurk M, Veski S. 2001. High-resolution analyses of an early Holocene climate event may imply decreased solar forcing as an important trigger. *Geology* **29**: 1107–1110.

Björck S, Koc N, Skog G. 2003. Consistently large marine reservoir ages in the Norwegian Sea during the Last Deglaciation. *Quaternary Science Reviews* **22**: 429–435.

Blaauw M, Christen JA. 2005. Radiocarbon and peat chronologies and environmental change. *Applied Statistics* **54**: 805–816.

Bond G, Kromer B, Beer J, Muscheler R, Evans MN, Showers W, Hoffmann S, Lotti-Bond R, Hajdas I, Bonani G. 2001. Persistent solar influence on north Atlantic climate during the Holocene. *Science* **294**: 2130–2136.

Broecker WS. 1998. Paleocean circulation during the last deglaciation: a bipolar seesaw? *Paleoceanography* **13**: 119–121.

Broecker WS. 2003. Does the trigger for abrupt climate change reside in the ocean or in the atmosphere? *Science* **300**: 1519–1522.

Buck CE, Christen JA, James GN. 1999. BCal: an on-line Bayesian radiocarbon calibration tool. *Internet Archaeology* **7**: http://intarch.ac.uk/journal/issue7/buck

Davies SM, Branch NP, Lowe JJ, Turney CSM. 2002. Towards a European tephrochronological framework for Termination 1 and the Early Holocene. *Philosophical Transactions of the Royal Society London* **360**: 767–802.

Davies SM, Wastegård S, Wohlfarth B. 2003. Extending the limits of the Borrobol Tephra to Scandinavia and detection of new early Holocene tephra. *Quaternary Research* **59**: 345–352.

Davies SM, Mortensen AK, Baillie MGL, Clausen HB, Grönvold K, Hall VA, Johnsen SJ, Pilcher JR, Steffensen JP, Wastegård S. 2004a. Tracing Volcanic Events in the Greenland Ice Cores. *PAGES News* **12**: 10–11.

Davies SM, Wohlfarth B, Wastegård S, Andersson M, Blockley S, Possnert G. 2004b. Were there two Borrobol Tephras during the early Lateglacial period: implications for tephrochronology? *Quaternary Science Reviews* **23**: 581–589.

Davies SM, Hoek WZ, Bohncke SJP, Lowe JJ, Pyne O'Donnell S, Turney CSM. 2005. Detection of Lateglacial distal tephra layers in the Netherlands. *Boreas* **34**: 123–135.

Dugmore AJ, Larsen G, Newton AJ. 1995. Seven tephra isochrones in Scotland. *The Holocene* **5**: 257–266.

Eiriksson J, Knudsen KL, Haflidason H, Henriksen P. 2000. Late-glacial and Holocene palaeoceanography of the North Icelandic shelf. *Journal of Quaternary Science* **15**: 23–42.

Goslar T, Arnold M, Tisnerat-Laborde N, Hatté C, Paterne M, Ralska-Jasiewiczowa M. 2000. Radiocarbon calibration by means of varves versus ^{14}C ages of terrestrial macrofossils from lake Gosciaz and Lake Perespilno, Poland. *Radiocarbon* **42**: 335–348.

Grimm EC. 1987. CONISS: a Fortran 77 program for stratigraphically constrained cluster analysis by the method of incremental sum of squares. *Computers and Geosciences* **13**: 13–35.

Grimm EC. 1991. *Tilia 1.12, Tilia Graph 1.18*. Illinois State Museum, Springfield.

Grimm EC. 1992. Tilia and Tilia-graph: Pollen spreadsheet and graphics program. *Programs and Abstracts, 8th International Palynological Congress, Aix-en-Provence*, September 8–12, 1992. American Association of Stratigraphic Palynologists: Texas; 56.

Grönvold K, Óskarsson N, Johnsen SJ, Clausen HB, Hammer CU, Bond G, Bard E. 1995. Ash layers from Iceland in the Greenland GRIP ice core correlated with oceanic and land sediments. *Earth and Planetary Science Letters* **135**: 149–155.

Gulliksen S, Birks HH, Possnert G, Mangerud J. 1998. A calendar age estimate of the Younger Dryas–Holocene boundary at Krakenes, western Norway. *Holocene* **8**: 249–259.

Haflidason H, Eiríksson J, van Kreveld S. 2000. The tephrochronology of Iceland and the North Atlantic region during the Middle and Late Quaternary: a review. *Journal of Quaternary Science* **15**: 3–22.

Hughen KA, Overpeck JT, Lehman SJ, Kashgarian M, Southon J, Peterson LC, Alley R, Sigman DM. 1998. Deglacial changes in ocean circulation from an extended radiocarbon calibration. *Nature* **391**: 65–68.

Hughen KA, Southon JR, Lehman SJ, Overpeck JT. 2000. Synchronous radiocarbon and climate shifts during the last deglaciation. *Science* **290**: 1951–1954.

Kitagawa H, van der Plicht J. 2000. Atmospheric radiocarbon calibration beyond 11,900 cal BP from Lake Suigetsu laminated sediments. *Radiocarbon* **42**: 369–380.

Lotter AF, Eicher U, Siegenthaler U, Birks HJB. 1992. Late-glacial climatic oscillations as recorded in Swiss lake sediments. *Journal of Quaternary Science* **7**: 187–204.

Lotter AF, Birks HJB, Zolitschka B. 1995. Late-glacial pollen and diatom changes in response to two different environmental perturbations: volcanic eruption and Younger Dryas cooling. *Journal of Paleolimnology* **14**: 23–47.

Lowe DJ, Hunt JB. 2001. A summary of terminology used in tephra-related studies. In *Tephras, Chronologie, Archéologie*, Juvigné E, Raynal JP (eds). Les dossiers de l'Archéo-Logis 1; 17–22.

Lowe JJ, Walker MJC. 2000. Radiocarbon dating the last glacial–interglacial transition (ca. 14–9 ^{14}C ka BP) in terrestrial and marine records: the need for new quality assurance protocols. *Radiocarbon* **42**: 53–68.

Lowe JJ, Birks HH, Brooks SJ, Coope GR, Harkness DD, Mayle FE, Sheldrick C, Turney CSM, Walker MJC. 1999. The chronology of palaeoenvironmental changes during the Last Glacial–Holocene transition: towards an event stratigraphy for the British Isles. *Journal of the Geological Society, London* **156**: 397–410.

Lowe JJ, Hoek WZ, INTIMATE group. 2001. Inter-regional correlation of palaeoclimatic records for the Last Glacial–Interglacial Transition: a protocol for improved precision recommended by the INTIMATE project group. *Quaternary Science Reviews* **20**: 1175–1187.

Lowe JJ, Walker MJC, Scott EM, Harkness DD, Bryant CL, Davies SM. 2004. A coherent high-precision radiocarbon chronology for the Late-glacial sequence at Sluggan Bog, Co. Antrim, Northern Ireland. *Journal of Quaternary Science* **19**: 147–158.

Moore PD, Webb JA, Collinson ME (eds). 1991. *Pollen Analysis*. Blackwell: Oxford; 1–216.

Mortensen AT, Bigler M, Grönvold K, Steffensen JP, Johnsen SJ. 2005. Volcanic ash layers from the Last Glacial Termination in the NGRIP ice core. *Journal of Quaternary Science* **20**: 209–219.

Pearce NJG, Westgate JA, Perkins WT, Preece SJ. 2004. The application of ICP-MS methods to tephrochronological problems. *Applied Geochemistry* **19**: 289–322.

Pilcher JR, Hall VA. 1992. Towards a tephrochronology for the Holocene of the north of Iceland. *The Holocene* **2**: 255–259.

Pilcher JR, Hall VA, McCormac FG. 1996. An outline tephrochronology for the Holocene of the north of Iceland. *Journal of Quaternary Science* **11**: 485–494.

Pilcher J, Bradley RS, Francus P, Anderson L. 2005. A Holocene tephra record from the Lofoten Islands, Arctic Norway. *Boreas* **34**: 136–156.

Possnert G. 1990. Radiocarbon dating by the accelerator technique. *Norwegian Archaeological Review* **23**: 30–37.

Ranner PH, Allen JRM, Huntley B. 2005. A new early Holocene cryptotephra from northwest Scotland. *Journal of Quaternary Science* **20**: 201–208.

Reimer PJ, Baillie MGL, Bard E, Bayliss A, Beck JW, Bertrand CJH, Blackwell PG, Buck CE, Burr GS, Cutler KB, Damon PE, Edwards RL, Fairbanks RG, Friedrich M, Guilderson TP, Hogg AG, Hughen KA, Kromer B, McCormac G, Manning S, Bronk Ramsey C, Reimer RW, Remmele S, Southon JR, Stuiver M, Talamo S, Taylor FW, van der Plicht J, Weyhenmeyer CE. 2004. IntCal04 Terrestrial Radiocarbon Age Calibration, 0–26 cal kyr BP. *Radiocarbon* **46**: 1029–1058.

Renssen H, van Geel B, van der Plicht J, Magny M. 2000. Reduced solar activity as a trigger for the start of the Younger Dryas. *Quaternary International* **71**: 373–383.

Rose NL, Golding PNE, Battarbee RW. 1996. Selective concentration and enumeration of tephra shards from lake sediment cores. *The Holocene* **6**: 243–246.

Turney CSM. 1998a. Extraction of rhyolitic component of Vedde microtephra horizons to correlate lake sediments. *Journal of Paleolimnology* **19**: 199–206.

Turney CSM. 1998b. *Isotope stratigraphy and tephrochronology of the last glacial–interglacial transition (14–9 ka ^{14}C BP) in the British Isles*. PhD thesis, University of London.

Turney CSM, Harkness DD, Lowe JJ. 1997. The use of microtephra horizons to correlate Late-glacial lake sediment successions in Scotland. *Journal of Quaternary Science* **12**: 525–531.

Turney CSM, Lowe JJ, Davies SM, Hall V, Lowe DJ, Wastegård S, Hoek W, Alloway B, SCOTAV members, INTIMATE members. 2004. Tephrochronology of Last Termination sequences in Europe: a protocol for improved analytical precision and robust correlation procedures (a joint SCOTAV–INTIMATE proposal). *Journal of Quaternary Science* **19**: 111–120.

van der Plicht J, van Geel B, Bohncke SJP, Bos JAA, Blaauw M, Speranza AOM, Muscheler R, Björck S. 2004. The Preboreal climate reversal and a subsequent solar-forced climate shift. *Journal of Quaternary Science* **19**: 263–269.

Walker MJC. 2001. Rapid climate change during the last glacial–interglacial transition; implications for stratigraphic subdivision, correlation and dating. *Global and Planetary Change* **30**: 59–72.

Walker MJC, Björck S, Lowe JJ, Cwynar LC, Johnsen S, Knudsen KL, Wohlfarth B. 1999. Isotopic 'events' in the GRIP ice core: a stratotype for the Late Pleistocene. *Quaternary Science Reviews* **18**: 1143–1150.

Wastegård S, Björck S, Possnert G, Wohlfarth B. 1998. Evidence for the occurrence of Vedde Ash in Sweden: radiocarbon and calendar age estimates. *Journal of Quaternary Science* **13**: 271–274.

Wastegård S, Turney CSM, Lowe JJ, Roberts SJ. 2000a. New discoveries of the Vedde Ash in southern Sweden and Scotland. *Boreas* **29**: 72–78.

Wastegård S, Wohlfarth B, Subetto DA, Sapelko TV. 2000b. Extending the known distribution of the Younger Dryas Vedde Ash into northwestern Russia. *Journal of Quaternary Science* **15**: 581–586.

Wohlfarth B, Possnert G, Skog G, Holmquist B. 1998. Pitfalls in the AMS radiocarbon-dating of terrestrial macrofossils. *Journal of Quaternary Science* **13**: 137–145.